AGU PUBLICATIONS

Water Resources Research

RESEARCH ARTICLE
10.1002/2014WR015639

Physical context for theoretical approaches to sediment transport magnitude-frequency analysis in alluvial channels

Joel Sholtes[1], Kevin Werbylo[1,2], and Brian Bledsoe[1]

[1]Department of Civil and Environmental Engineering, Colorado State University, Fort Collins, Colorado, USA, [2]Water Resources Engineer, Headwaters Corporation, Denver, Colorado, USA

Key Points:
- We test and expand on theoretical approach to sediment magnitude-frequency analysis
- PDFs representing river flow overweight effectiveness of infrequent flows
- Adding complexity to theoretical approach helps explain empirical findings

Correspondence to:
J. Sholtes,
jsholtes@gmail.com

Citation:
Sholtes, J., K. Werbylo, and B. Bledsoe (2014), Physical context for theoretical approaches to sediment transport magnitude-frequency analysis in alluvial channels, *Water Resour. Res.*, *50*, doi:10.1002/2014WR015639.

Received 31 MAR 2014
Accepted 15 SEP 2014
Accepted article online 17 SEP 2014

Abstract Theoretical approaches to magnitude-frequency analysis (MFA) of sediment transport in channels couple continuous flow probability density functions (PDFs) with power law flow-sediment transport relations (rating curves) to produce closed-form equations relating MFA metrics such as the effective discharge, Q_{eff}, and fraction of sediment transported by discharges greater than Q_{eff}, $f+$, to statistical moments of the flow PDF and rating curve parameters. These approaches have proven useful in understanding the theoretical drivers behind the magnitude and frequency of sediment transport. However, some of their basic assumptions and findings may not apply to natural rivers and streams with more complex flow-sediment transport relationships or management and design scenarios, which have finite time horizons. We use simple numerical experiments to test the validity of theoretical MFA approaches in predicting the magnitude and frequency of sediment transport. Median values of Q_{eff} and $f+$ generated from repeated, synthetic, finite flow series diverge from those produced with theoretical approaches using the same underlying flow PDF. The closed-form relation for $f+$ is a monotonically increasing function of flow variance. However, using finite flow series, we find that $f+$ increases with flow variance to a threshold that increases with flow record length. By introducing a sediment entrainment threshold, we present a physical mechanism for the observed diverging relationship between Q_{eff} and flow variance in fine and coarse-bed channels. Our work shows that through complex and threshold-driven relationships sediment transport mode, channel morphology, flow variance, and flow record length all interact to influence estimates of what flow frequencies are most responsible for transporting sediment in alluvial channels.

1. Introduction

To what discharge or range of discharges does a river adjust its dimensions to balance the inputs of flow and sediment while maintaining a dynamically stable form? This question underlies research conducted by generations of geomorphologists and engineers on the relationship between alluvial channel form, sediment transport, and flow regime [e.g., *Mackin*, 1948; *Wolman and Miller*, 1960; *Pickup and Warner*, 1976; *Hey and Thorne*, 1986; *Emmett and Wolman*, 2001; *Doyle et al.*, 2007]. Alluvial channels are those with boundaries that adjust in response to erosion and deposition of sediment. *Wolman and Miller* [1960] introduced the hypothesis that the theoretical channel-forming discharge is some intermediate, near-bankfull discharge that, over time, performs the most work (i.e., transports the most sediment). They define this discharge as the most "effective" discharge, Q_{eff}. Since then, scores of studies searching for a relationship between channel form and Q_{eff} have been published. Some workers have found a strong (e.g., 1:1) relationship between the bankfull discharge, Q_{bf}, and Q_{eff} [*Andrews*, 1980; *Andrews and Nankervis*, 1995; *Hey*, 1996; *Emmett and Wolman*, 2001; *Torizzo and Pitlick*, 2004] while others have found a wide range of variability in the $Q_{bf} - Q_{eff}$ relationship [*Pickup and Warner*, 1976; *Nolan et al.*, 1987; *Soar and Thorne*, 2001]. Nevertheless, the concept of effective discharge—and the analytical framework of magnitude and frequency analysis of sediment transport—has provided a valuable tool for examining relationships between channel form and process.

Much work has been conducted to operationalize and standardize empirical magnitude-frequency analysis (MFA) for use on rivers and streams with flow records and measured or modeled sediment transport [e.g., *Benson and Thomas*, 1966; *Biedenharn et al.*, 2000]. Empirical MFA involves representing a daily or subdaily flow record as an empirical probability distribution through either binning the flows in a histogram [*Biedenharn et al.*, 2000; *Soar and Thorne* 2001] or numerically differentiating the empirical cumulative distribution function of the flows [*Orndoff and Whiting*, 1999]. This empirical probability distribution is then multiplied

by a sediment transport-discharge relation, which may either be a statistical regression, or a site-calibrated sediment transport equation [e.g., *Hey*, 1996] to create an empirical effectiveness histogram or curve.

While *Wolman and Miller* [1960] originally suggested that a continuous, theoretical probability density function (PDF) could be used to represent the flow regime, it was not until three decades later that this theoretical approach to MFA was formalized [*Nash*, 1994; *Vogel et al*., 2003; *Goodwin*, 2004; *Quader and Guo*, 2009; *Klonksy and Vogel*, 2011]. The theoretical approach to MFA involves multiplying an assumed continuous PDF or one that is fit to the flow distribution (e.g., the lognormal or gamma distribution) with a sediment-transport relation, which may be as simple as a power law function that relates sediment transport to flow, or a more complex and threshold driven relation. Metrics based on the resulting effectiveness curve equation may then be derived by analytical integration. The appeal of the theoretical approach to MFA lies in the ability to generate easily applied, closed-form solutions to MFA metrics such as Q_{eff} [*Goodwin*, 2004] and the amount of sediment transported by discharges greater than Q_{eff}, $f+$ [*Vogel et al*., 2003]. With these, one can expediently determine the relationship between MFA metrics, and attributes of the flow regime (e.g., coefficient of variation, skewness, etc.) and/or sediment transport mode (e.g., empirical sediment rating curve exponent, and critical shear stress for bed mobilization). Furthermore, one could use these relations to predict how a channel might respond to a change in flow variability or sediment supply due to environmental change assuming a correlation between Q_{eff}, or another MFA metric, and Q_{bf}.

Using the theoretical approach, *Vogel et al*. [2003] found that Q_{eff} often takes on a relatively low value (and $f+$ a large value) and is responsible for relatively little load transport over time while larger, less frequent discharges are often responsible for the majority of load transport in rivers. They argue that Q_{eff} may not be a useful metric when considering what flows are responsible for transporting the bulk of suspended sediment in a channel. It should be noted that *Vogel et al*. [2003] were more interested in total river load in general (solutes, suspended sediment, etc.), and not specifically in geomorphically significant flows. From a geomorphic perspective, many empirical MFA studies have found correspondence between Q_{eff} and Q_{bf}, suggesting that some relationships exist between the discharge range that maximizes the effectiveness of sediment transport and channel form in certain channel types [*Wolman and Miller*, 1960; *Andrews*,1980; *Carling*, 1988; *Hey*, 1996; *Emmett and Wolman*, 2001]. Here, we explore why theoretical and empirical approaches can produce contradictory results.

The present study takes a dualistic approach to investigate claims on the magnitude and frequency of sediment transport in channels based on theoretical, closed-form solutions to MFA metrics. We utilize the analytical framework of the theoretical approaches to study how adding complexity to them changes the predicted relationships between flow regime, sediment transport mode, and MFA metrics. For this first objective, we begin by considering the influence of flow and sediment transport mode on MFA metrics using the original theoretical approaches (sections 3.1 and 4.1). As discussed above, we acknowledge the limitations of these approaches; however, we find it illustrative to begin this study by exploring the relationships they produce. To add complexity to these approaches, we introduce a compound channel form (sections 3.3 and 4.3) and a threshold for sediment entrainment (sections 3.4 and 4.4) and consider the influence of flow variability and sediment transport mode on MFA metrics calculated from these updated theoretical approaches. For the second objective, we test the assumptions of the theoretical approaches themselves by considering how MFA metrics calculated from theoretical approaches, which use continuous PDFs to represent the flow record, compare with those calculated with a synthetic empirical approach using discrete, finite, flow records sampled from those same PDFs (sections 3.2 and 4.2).

We begin with a more thorough introduction to theoretical MFA approaches and outline our methods for accomplishing the objectives stated above. We end with a discussion of how and why results from theoretical and empirical approaches diverge. We also explore how theoretical approaches can be extended to incorporate a higher degree of physical realism, which in turn allows them to be used to evaluate more complex relationships between channel form and the magnitude and frequency of sediment transport.

2. Theoretical Framework

This investigation follows and expands upon the analytical framework of previous theoretical MFA work [*Nash*, 1994; *Vogel et al*., 2003; *Goodwin*, 2004]. Consistent with this previous work, we initially represent the sediment transport-discharge relationship as a power law: $Q_s = \alpha Q^{\beta}$, where Q_s has units of mass/time,

specifically (tonnes/day). In this sediment rating, curve α is a scaling coefficient that is positively related to the magnitude of sediment flux and drainage area [*Syvitski et al*., 2000; *Barry et al*., 2004]. Implicit in this rating curve is a discharge-bed shear stress relationship. It has been shown that the value of α does not affect the value of Q_{eff} or other normalized MFA metrics [*Nash*, 1994; *Goodwin*, 2004], so it will not be specifically considered in this study. The rating curve exponent, β, is positively correlated to the size of the largest bed particles (D_{84}) [*Emmett and Wolman*, 2001], bed armoring [*Barry et al*., 2004], and dependent upon sediment transport measurement technique [*Bunte et al*., 2004], as well as channel morphology (i.e., stage-discharge relationship) [*Hey*, 1996] among other factors.

The mechanisms by which sediment moves through a channel (e.g., in suspension or along the bed) should inform the type of transport relation used. Where sediment transport measurements exist, a statistical regression may be used, often taking the form of a power law function (sediment rating curve). Where empirical sediment rating curves are not available, semiempirical, sediment transport relations, calibrated to the hydraulics and sediment of the channel of interest, are relied upon. *Barry et al*. [2008] found that the calculated value of Q_{eff} is insensitive to the type of transport equation used in bed load channels.

Many continuous probability distribution functions have been used to represent daily stream flow, which are generally highly positively skewed, including the two-parameter lognormal, gamma, Generalized Pareto, exponential, as well as broken power law functions [e.g., *Vogel et al*., 2003; *Goodwin*, 2004; *Archfield et al*., 2007; *Quader and Guo* 2009; *Segura and Pitlick*, 2010]. In general, continuous PDFs fit natural flow records with mixed results, especially in the right tail of the distribution and in multimodal cases [*Nash*, 1994; *Segura and Pitlick*, 2010]. *Nash* [1994] found that on large rivers the lognormal distribution fit daily flows well in some circumstances and poorly in others due to the multimodal nature of some flow records, as well as skewness and kurtosis combinations that exceeded what is possible with the lognormal distribution. *Quader and Guo* [2009] tested the fit of the exponential distribution on daily flows, finding that it performs the best in smaller streams but found poor fits between flow records and continuous PDFs in general, especially among streams with intermittent flow. *Segura and Pitlick* [2010] found that a broken power law function better fit the frequency distribution of daily flows in snowmelt-dominated streams, as compared to the exponential and lognormal distributions. While it does not fit daily flow distributions well in some cases, we chose to work with the two-parameter lognormal distribution function due to its demonstrated ability to represent skewed daily stream flow distributions in many cases [*Limbrunner et al*., 2000], its relative parsimony, and its historical use in generating theoretical MFA relationships [*Wolman and Miller*, 1960; *Nash*, 1994; *Vogel et al*., 2003; *Goodwin*, 2004].

$$f(Q)=\frac{1}{Q\sqrt{2\pi\sigma_y^2}}\exp\left\{-\frac{1}{2\sigma_y^2}\left[\ln(Q)-\mu_y\right]^2\right\} \quad (1)$$

Here, Q represents the average daily flow value (m^3/s), and μ_y and σ_y are the mean and standard deviation of the logarithm of the average daily flows, respectively. Using other skewed, continuous PDFs such as the gamma distribution produced qualitatively similar theoretical relationships as the lognormal distribution. It is possible for the exponential distribution to have a relatively thick right tail for large values of C_v when fit using the method of moments. This can lead to a negative relationship between $f+$ and C_v (opposite of the relationship produced using lognormal or gamma PDFs); however, such thick right tails may not be realistic for natural flow regimes. Also, it should be noted that a subdaily time resolution may be more appropriate for analyzing sediment yield in rivers whose discharge may vary widely within a day such as those with small drainage areas and flashy hydrology [*Biedenharn et al*., 2000]; however, for the purposes of this study, we only consider flow regimes with daily time resolution.

Flow records are samples of the underlying population distribution of the flow regime and are discrete and finite in nature. This is particularly evident in the right tail of the distribution where continuous PDFs may overrepresent the discrete, sporadic occurrence of infrequent flood events. Even if a flow record perfectly represents a sample from a certain probability density function, an infinite sample size would be required before the empirical PDF would match the shape of theoretical PDF. As the period of record length increases past 50–100 years and beyond, assumptions of channel equilibrium and flow regime stationarity inherent in MFA may be violated. As such, continuous PDFs will always approximate finite flow records due to their discrete nature. Nevertheless, results from MFA using continuous PDFs can yield important insights

about the relationships between flow regime and the magnitude and frequency of sediment transport [*Vogel et al*., 2003; *Goodwin*, 2004; *Quader and Guo*, 2009; *Klonsky and Vogel*, 2011].

Vogel et al. [2003] and *Goodwin* [2004] demonstrate that a closed-form solution for the effective discharge can be derived by multiplying a continuous PDF with a sediment-rating curve to create the effectiveness curve. The flow that coincides with the peak of the effectiveness curve, found by taking its derivative, is known as the effective discharge. The resulting expression is a parsimonious, closed-form function of the rating curve exponent, β, and the mean and variance of the logarithms of daily flow when the lognormal PDF is used:

$$Q_{eff} = \exp\left[\mu_y + \sigma_y^2(\beta - 1)\right] \tag{2}$$

Many methods exist to calculate the value of Q_{eff} directly—or empirically—from a flow record and either a measured sediment-rating curve or calibrated sediment transport relation [e.g., *Hey*, 1996; *Biedenharn et al*., 2000; *Soar and Thorne*, 2001]. Generally, Q_{eff} is equal to the median value of the discharges contained in the maximum effectiveness histogram bin, which is the product of a daily flow histogram and the sediment transport relation. It can also be determined with an empirical kernel density function [*Klonsky and Vogel*, 2011] or as the maximum finite difference derivative of the empirical cumulative distribution form of the effectiveness curve [*Orndorff and Whiting*, 1999].

Based on the lognormal distribution for daily flows, the return interval in years of Q_{eff} is:

$$RI = \frac{1/365}{1 - \Phi\left[\frac{\ln(Q_{eff}) - \mu_y}{\sigma_y}\right]} \tag{3}$$

where the expression $\Phi[\,]$ represents the standard normal cumulative distribution function (CDF) [*Vogel et al*., 2003]. Here, *RI* represents the return interval in years calculated from the daily flow series PDF. We do not use a nonparametric or empirical alternative to equation (3) in this study because we are sampling from the lognormal distribution. Additionally, *Vogel et al*. [2003] derived a closed-form solution for the fraction of average total sediment load transported by discharges greater than Q_{eff}, $f+$:

$$f+ = 1 - \Phi\left[-\sqrt{\ln(1 + C_v^2)}\right] \tag{4}$$

where C_v is the coefficient of variation of the untransformed daily flows (σ_x/μ_x). This function monotonically increases with C_v with an asymptote at unity. The empirical analog to the theoretical approach simply involves dividing the total amount of sediment transported on each day summed over a flow record by the amount of sediment transported by flows greater than Q_{eff}.

3. Data and Methods

3.1. Flow Regime Analysis

We begin by considering the range of variance in natural flow regimes. *Poff* [1996] conducted an analysis of the statistical properties of daily flows in unregulated streams and rivers in the conterminous United States. He created flow regime categories by grouping rivers by various statistical properties. We select several of his flow regime categories representing the range of variance he reports from groundwater and snowmelt-driven hydrology to flashy and intermittent hydrology ($1 < C_v < 5$). To understand how flow regime variance—represented by the coefficient of variation of the average daily flow—affects the magnitude and frequency of sediment transport, we solve equations (2), (3), and (4) for this range of values of C_v. We also use this range of C_v values to inform the subsequent analyses.

3.2. Flow Record Length

Our first test of the theoretical approach to magnitude frequency analysis (MFA) compares values and return intervals of Q_{eff} and values of $f+$ generated from equations (2), (3), and (4) with those generated from synthetic daily flow records of varying length (10, 100, 1000, and 100,000 years) sampled from the lognormal distribution. We create these extremely long flow records (large sample sizes) to examine how empirical MFA metrics compare to theoretical values as the flow record sample approaches the continuous, underlying population distribution (the lognormal PDF) used in the theoretical approach. Using 1000–100,000 year records will increase the probability of sampling a large and rare event, but these large events

will receive less weight in the empirical density function for large sample sizes, and hence less influence on MFA. In fact, a large flood sampled in a short flow record, will have an overwhelming influence on MFA because it will receive more weight in the histogram (higher density) due to the smaller sample size. To generate synthetic daily flow records for each combination of C_v value (0.5–5) and flow record length (*RL*) considered, we used a uniform distribution to randomly sample the two-parameter lognormal CDF specified by a constant mean (μ_x) of 2 m^3/s (arbitrary value) and C_v values ranging from 0.5 to 5. For each flow record length, we created 100 trials of *RL**365 random samples from the lognormal CDF for every value of C_v. The mean and variance of the lognormal distribution are calculated by the method of moments where the values in parentheses are untransformed [*Yevjevich*, 2010]:

$$\mu_y = \frac{1}{2}\ln\left(\frac{\mu_x^2}{1+C_v{}^2}\right) \tag{5}$$

$$\sigma_y^2 = \ln\left(1+C_v{}^2\right) \tag{6}$$

Next, we created an empirical flow PDF or histogram of the synthetic flow record. Much consideration has been given to the number of histogram bins and method for calculating the bin intervals in effective discharge analysis with suggestions ranging from 25 to 100 equally spaced (arithmetic) discharge classes and discouraging the use of logarithmic classes [*Biedenharn et al*., 2000; *Soar and Thorne*, 2001]. More rigorous statistical approaches have been suggested by *Orndoff and Whiting* [1999] who use a numerical differentiation of the empirical flow CDF, and *Klonksy and Vogel* [2011] who recommend using a kernel density function. For simplicity, we use the general approach outlined by *Biedenharn et al*. [2000]. We modify their method slightly to best represent flow record lengths ranging from 10 to 100,000 year by using a constant 50 equally space arithmetic bins to create histograms of daily flow. Additionally, we do not modify the width of discharge bin classes such that no bins contain zero flows as per Biedenharn et al. [2000]. Sensitivity analysis indicates that relative relationships among the MFA metrics and C_v, β, and *RL* variables are not affected by the number of bins (bin width) used for $25 \leq \#\ of\ bins \leq 100$. The midpoints of each histogram bin are then multiplied by sediment-rating curves of the form $Q_s = \alpha Q^{\beta}$ to generate the synthetic "empirical" effectiveness histograms. The median value of all the daily discharges contained in the maximum effectiveness histogram bin represents the effective discharge.

The coefficient of the rating curve, α was arbitrarily set to 0.02. The value of α does not affect the value of Q_{eff} [*Nash*, 1994; *Goodwin*, 2004] or normalized MFA metrics such as $f+$; therefore, keeping this value constant and arbitrary was deemed reasonable. We consider values of the exponent β from 0.5 to 5. This range represents the spectrum of observed sediment-rating curve exponent values where smaller values as low as 1 are generally associated with suspended sediment transport [*Nash*, 1994; *Syvitski et al*., 2000]. Values less than 1 are uncommon. Larger values of β up to and greater than 5 are generally associated with bed load transport [*Emmett and Wolman*, 2001; *King et al*., 2004; *Pitlick et al*., 2009]. These ranges are not exhaustive; indeed, values of β up to and greater than 10 have been reported for bed load transport in mountain streams with relatively low transport stages [*Bunte et al*., 2004]. However, the range of β selected for this study serves to illustrate the relationship between sediment transport mode, as represented by the rating curve exponent, β, over the range of flow regimes.

We summarize the empirical MFA metric results as a function of C_v, β, and *RL* by reporting median values from the 100 trials. Increasing the number of trials from 100 to 1000 and 10,000 does not significantly alter the median value of the MFA metrics, nor does it influence the trends and relationships reported here.

3.3. Compound Channel Form

Next, we compare theoretical approaches to MFA derived from the single power law (SPL) sediment-rating curve function—equations (2) to (4)—to those generated using a piecewise or broken power law (BPL) function that represents a compound channel form consistent with many natural channel cross sections. Compound channels exhibit a break in lateral slope between the channel and the floodplain and hence a break in transport effectiveness [*Hey*, 1996] (Figure 1). We consider how flow variance interacts with compound channel form to drive sediment transport effectiveness.

We use an at-a-station hydraulic geometry relation of the form $h = aQ^b$ to relate flow depth, *h*, to discharge for both in channel and overbank flows. Values of *a* and *b* were chosen to generally reflect reported values for in-channel hydraulic geometry relations [*Knighton*, 1998, p. 173]. We set the value of the in-channel

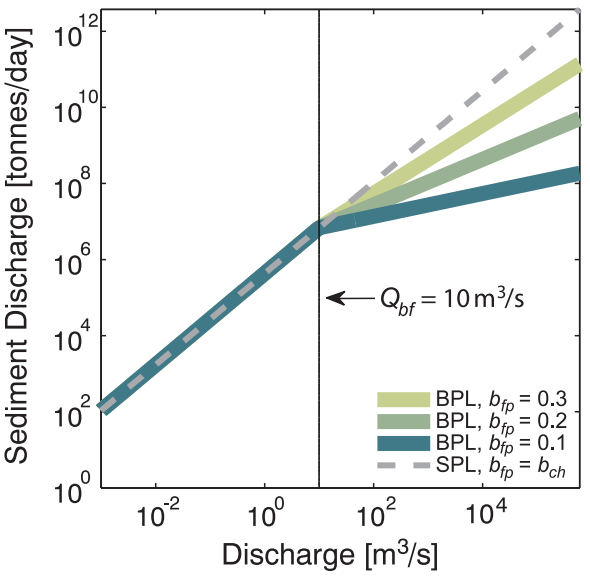

Figure 1. Log linear sediment-rating curves for single power law (SPL, broken line) and broken power law (BPL, solid lines) at-a-station hydraulic geometry relationships for in-channel (left of vertical line) and overbank flows (right of vertical line) with varying degrees of floodplain lateral slope.

coefficient, a_{ch}, to 0.2 and the value of the exponent, b_{ch}, was set to 0.4. To maintain continuity from in-channel to overbank flows, the value of the coefficient for overbank flows, a_{fp}, is a function of the coefficient for in-channel flows, as well as the exponents for both overbank and in-channel flows: $a_{fp}=a_{ch}Q_{bf}^{\left(b_{ch}-b_{fp}\right)}$, where Q_{bf} is the bankfull discharge. For this analysis, Q_{bf} was arbitrarily chosen to be 10 m^3/s, consistent with an intermediately sized channel. We vary the value of the overbank flow exponent, b_{fp}, from 0.1 to 0.3 to test the sensitivity of the analysis to the difference in lateral slope between the channel banks and the floodplain. These at-a-station hydraulic geometry parameter values for overbank flows correspond to those reported for stage-discharge relationships in compound channels elsewhere [*Ackers*, 1993; *Shiono et al.*, 1999]. We use downstream hydraulic geometry relations to calculate channel width and slope as a function of Q_{bf} developed from coarse-bedded streams in the Rocky Mountains, Colorado by *Torrizo and Pitlick* [2004].

The statistical properties of the flow regime must be related to Q_{bf} in a nonarbitrary manner. That is, the flow regime must "fit" the channel geometry represented by the value of Q_{bf}. To do this, we used a single log linear regression between mean annual discharge and Q_{bf} ($n = 10$, $R^2 = 0.92$) from the streams studied by *Torrizo and Pitlick* [2004]:

$$\mu_x=0.151Q_{bf}^{0.873} \tag{7}$$

The relationship between mean daily discharge and Q_{bf} used in this analysis is unique to the Colorado Rocky Mountains where it was developed. As before, we maintain μ_x constant and vary C_v from 0.5 to 5. We acknowledge that flow regime variability can influence channel form. Varying flow variability while maintaining a constant channel form is a simplification used in this study.

The single power law sediment-rating curve assumes a single stage discharge relationship. To incorporate a compound channel form, we use a simplified, nonsediment entrainment threshold version of the Einstein-Brown (EB) equation as reported in *Brown* [1950] because it has a form similar to a power law sediment-rating curve:

$$Q_s=k_1\tau_*^3 \quad \tau_*=\frac{hS}{(G-1)D_s} \tag{8}$$

In equation (8), k_1 is a constant coefficient, which converts dimensionless unit width, volumetric sediment flux to total sediment discharge (tonnes/day), G is the specific gravity of the sediment (set to 2.65), and D_s is the characteristic sediment diameter. The independent variable in this equation, τ^*, is the dimensionless Shields parameter, which is a linear function of depth, h for wide rectangular channels, and friction slope, S. Hence, with depth defined as a power law function of discharge, and Q_s defined as a power law function of τ^*, Q_s in (8) can now be defined as a power law function of discharge. This is a continuous relationship in the SPL case and a broken or piecewise relationship in the BPL case. Results using (8) can be directly compared to the power law sediment-rating curve of the form $Q_s = \alpha Q^{\beta}$ used in theoretical MFA approaches:

$$Q_s=\frac{k_1a^3S^3}{\left[(G-1)D_s\right]^3}Q^{3b} \tag{9}$$

where a and b are equal to a_{ch} and b_{ch} for $Q \le Q_{bf}$ and equal to a_{fp} and b_{fp} for $Q > Q_{bf}$. We arbitrarily chose a grain size of 10 mm (medium gravel) for this analysis. Sensitivity analysis demonstrates that magnitude-

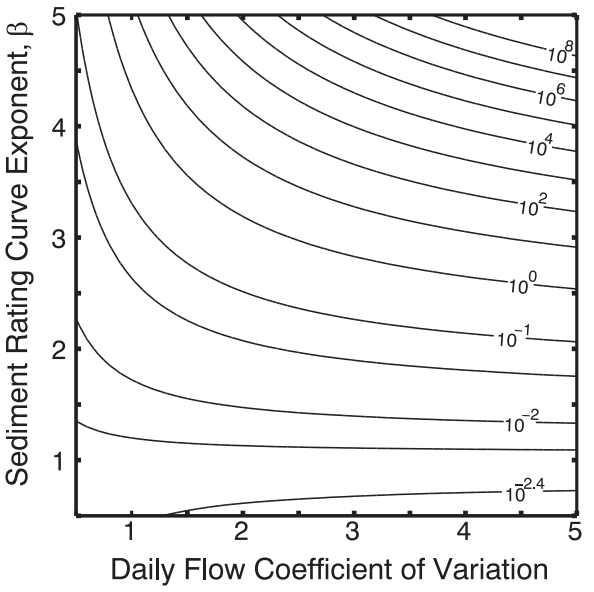

Figure 2. Return interval (year) of Q_{eff} for $\mu_x = 2$ m^3/s as a function of β and C_v.

frequency analysis metrics are not sensitive to the grain size using this simplified EB relation. We chose this form of sediment transport relation because it represents the sediment transport-discharge relationship in a nonarbitrary manner and can be directly compared to SPL-based theoretical MFA metrics as shown in equation (9) (Figure 1).

The majority of previous work has found the value of Q_{eff} to be less than or equal to Q_{bf} in alluvial channels [*Pickup and Warner*, 1976; *Andrews and Nankervis*, 1995; *Soar and Thorne*, 2001] with the exception of *Bunte et al*. [2013]. In the present analysis, Q_{eff} was always less than Q_{bf}, therefore the only MFA metric that was affected by the BPL sediment flux-discharge relationship was the fraction of sediment transported above Q_{eff}, $f+$. We generate effectiveness curves using finite approximations of the continuous lognormal PDF. To compare values of $f+$ for the SPL and BPL scenarios directly, we use the area under the SPL effectiveness curve as the denominator of $f+$.

3.4. Sediment Entrainment Threshold

In section 3.3, we considered the influence of compound channel form on MFA metrics without considering a threshold for sediment entrainment. Here we explore how the presence or absence of a threshold affects the values of MFA metrics compared to those derived by equations (2), (3), and (4). Using the same numerical analysis framework in section 3.3, we introduce a final sediment transport relation that includes a threshold for sediment entrainment: the Meyer-Peter and Müller (MPM) relation for uniformly sized sediment in transport as bed load [*Meyer-Peter and Müller*, 1948].

$$Q_s = k_2(\tau_* - \tau_{c*})^{1.5} \tag{10}$$

The constant, k_2, is similar in concept and units to k_1. Additionally, τ_c* represents the critical value of dimensionless shear stress for sediment entrainment (set to 0.047). It is a threshold value of dimensionless shear stress below which no sediment transport occurs. We chose MPM because it of its parsimony, which serves this illustration of the influence of a threshold of sediment transport on MFA metrics. Similar trends between MFA metrics and C_v result when a more complex bedload equation is used [e.g., *Parker*, 1979].

We vary the size of sediment considered from 1 mm (coarse sand) to 64 mm (very coarse gravel), which, for a given channel geometry, increases the flow depth and discharge necessary for sediment entrainment. Using MPM (10), and finite approximations of lognormal PDFs representing daily flows with C_v values ranging from 0.5 to 5, we generate finite approximations of theoretical effectiveness curves as before. We calculate values of the MFA metrics using MPM rather than a sediment-rating curve with no threshold for sediment transport (e.g., sections 3.1–3.3) and compare these with values from their theoretically derived counterparts.

4. Results and Discussion

4.1. Flow Regime Analysis

We begin with results from the theoretically derived MFA metrics from equations (2), (3), and (4) coupled with the flow regimes described above fit to lognormal PDFs. The relationship between *RI* as a function of β and C_v indicates that as β increases, *RI* increases for constant C_v, but more so for $C_v > 2$ (Figure 2). As C_v increases with constant β, *RI* increases for $\beta > 2$ (representative of the bed load-dominated domain), and is relatively constant for $\beta < 2$.

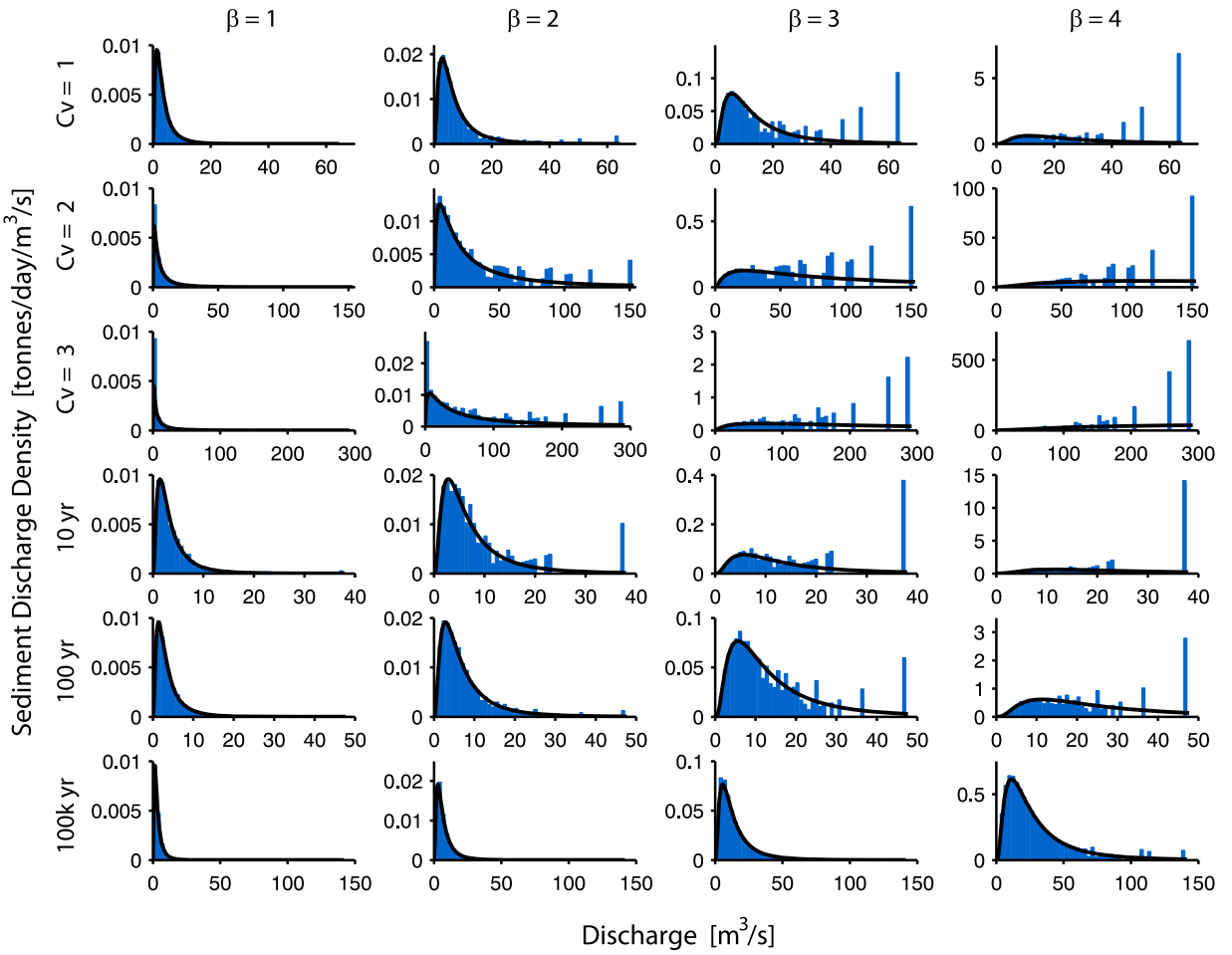

Figure 3. A random sample of effectiveness histograms for a range of β and C_v values for a 100 year flow record (top three rows) and a range of record lengths for $C_v = 1$ (bottom three rows) along with theoretical lognormal effectiveness curve (solid black curve). Flow samples are identical moving across columns. Flow samples change moving down rows as C_v and record length increase. Note that for $\beta \geq 3$, the largest discharge bin generally becomes the most effective. This is more apparent for larger values of C_v and for shorter flow record lengths.

The theoretical relation plotted in Figure 2 precludes the possibility of *RI* approximating the 1.5 year flow event for $\beta \leq 2.5$. The 1.5 year event is often cited as the median or average return interval for Q_{eff} or Q_{bf} though with questionable merit as discussed by *Doyle et al.* [2007]. While these general trends may translate to physical systems in some cases, the absolute values of *RI* shown in Figure 2 diverge from those reported for North American streams, calculated using empirical methods, which generally fall in the range of 0.5–2 years [*Pickup and Warner*, 1976; *Andrews*, 1980; *Nash*, 1994; *Emmett and Wolman*, 2001]. However, recent work by *Bunte et al.* [2013] using different bed load measurement techniques suggests that in coarse-bedded streams with very large sediment-rating curve exponents ($\beta > 5$), the largest flows are likely the most effective over time. While this theoretical relation may provide information about the general relationships between sediment transport mode, flow variance, and the magnitude of Q_{eff}, it is limited in its applicability to the physical world, especially for large β and C_v values.

As described by equation (4), $f+$ increases in an asymptotic manner with C_v and is not a function of β (see section 4.3 for further discussion). As C_v increases, the flow PDF and effectiveness curve become more positively skewed and the tails heavier. In other words, smaller discharges become more frequent and large discharges become slightly more frequent. This translates to a value of Q_{eff} that decreases with increasing C_v, in a relative sense. That is, Q_{eff} occupies an increasingly smaller position of cumulative sediment transport and the area of the effectiveness curve to the left of Q_{eff} decreases while the value of $f+$ increases (see section 4.4). In their analysis of sand bed streams, *Soar and Thorne* [2001] found an increasing relationship between $f+$ and a metric for flow variance; however, work by *Bunte et al.* [2013] in coarse-bedded streams

suggests otherwise. We explore this divergence in sediment transport and MFA metric behavior between fine and coarse-bed streams in section 4.4, below.

4.2. Flow Record Length Analysis

In the previous section, we considered the influence of C_v on MFA metrics using theoretical approaches alone, which use continuous PDFs to represent daily flows. Here we compare values of MFA metrics generated from theoretical approaches with those generated from synthetic, finite flow records sampled from the same underlying daily flow PDF (empirical approach). We begin this discussion by considering samples of effectiveness histograms representing a range of β and C_v values and flow record lengths (Figure 3). The effectiveness histograms plotted in Figure 3 (top three rows) represent a single 100 year flow record chosen randomly from the 100 trials conducted for each plotted value of C_v. As both β and C_v increase, larger, less frequent flows transport relatively more sediment over time. The effective discharge, or the median value of the flows in the bin with the maximum effectiveness value, tends to fall in the first flow bin for $C_v > 1$ and $\beta < 2$. The effective discharge tends to fall in the last flow bin for $\beta \geq 3$ over all values of C_v. At some threshold value of β, Q_{eff} jumps from a very frequent flow value to a very infrequent value in the right tail of the effectiveness histogram, sometimes falling in the last flow bin. This jump, or threshold, can be seen in the contour plots of $f+$ and *RI*, plotted as functions of β and C_v (Figure 4).

The number of years in a flow record also plays a role in the relationships between β and C_v and the MFA metrics $f+$ and *RI*. Consider effectiveness histograms generated from flow records with $C_v = 1$ and lengths varying from 10 to 100,000 years (Figure 3, bottom three rows). As the flow record length increases, the synthetic daily flow histogram more closely replicates the continuous function that is the product of the sediment-rating curve and the lognormal flow PDF underlying theoretical MFA approaches. This gives more weight to more frequent flows near the flow distribution peak. Less frequent flows in the tails of the distribution carry more weight in shorter flow records, which have fewer flows in each bin. This effect becomes more pronounced in the effectiveness histograms as the value of β increases for shorter flow records (Figure 3). The effective discharge calculated from shorter flow records is more sensitive to the occurrence of a rare flow event overwhelming sediment yield.

We continue this record length analysis by considering the relationship between MFA metrics $f+$ (Figure 4 top row) and *RI* (Figure 4 bottom row) as a function of β and C_v. Moving from bottom to top in each subplot in the upper row of Figure 4, $f+$ increases with β to a maximum value at $\beta \approx 1.8$ for the 10 year flow record up to $\beta \approx 3.8$ for the 100,000 year flow record. After this β threshold is reached, $f+$ drops precipitously to nearly zero when Q_{eff} falls into the largest discharge bin in the effectiveness histogram (see Figure 3). As β continues to increase, more weight is given to infrequent flows in the right hand tails of the flow probability distribution resulting in more sediment being transported at larger discharges (some greater than Q_{eff}) and a slow increase in $f+$ occurs after this threshold. The threshold described here begins at $\beta \approx 2.4$ for the 10 year records up to $\beta > 5$ for the 100,000 year records at $C_v = 0.5$ and decays to a constant $\beta \approx 1.8$ to 3.8 at C_v values that range from approximately 2.1 to 1.8 for the 10 years and 100,000 year record lengths, respectively.

The value of $f+$ is less sensitive to C_v than to β. In the case of relatively shorter flow records (e.g., 10–100 years), a more sparse distribution of flows allows a few large, infrequent flows to overwhelm the total sediment transport at smaller values of β. In the realm of existing flow record lengths (10–100 years), the behaviors of $f+$ and *RI* as functions of β and C_v transition smoothly from the values shown in Figure 4 for the 10–100 year plots.

The theoretical relation for $f+$ described by equation (4) is only a function of C_v and does not resemble the behavior plotted in Figure 4 (top row). A horizontal line at intermediate values of β (below the threshold) tracks the approximate trend described by equation (4) of $f+$ increasing asymptotically to unity with increasing C_v. The difference between the two descriptions of $f+$ lies in the difference between discrete flow series and flow series represented by continuous PDFs, as well as the definition of Q_{eff}. Even though the discrete, synthetic flow series generated for this study are derived from the same underlying PDF as equations (2) to (4), they behave differently than continuous PDFs in MFA in large part due to the lack of a continuous right tail in the flow distribution (histogram) of finite records (Figure 3). This lack of continuity in the tail of empirical records of course depends on sample size. Assuming, for example, that a river's flow regime perfectly fits the lognormal distribution, given a long enough period, the discrete flow record will

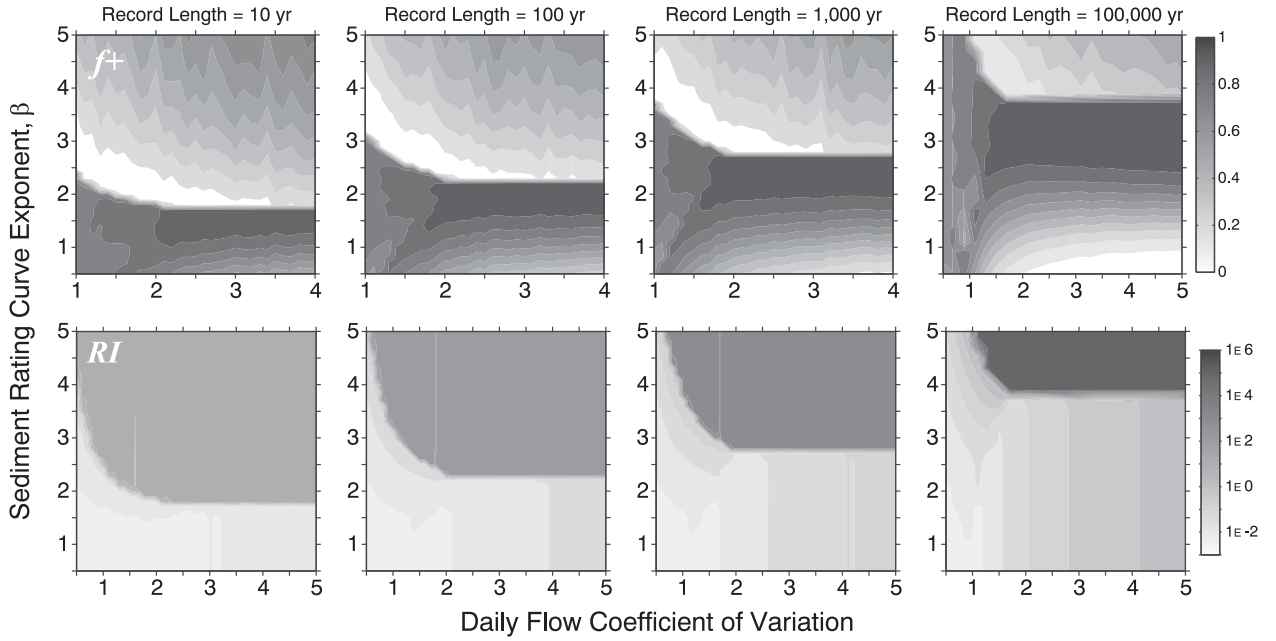

Figure 4. Contour plots of values of the fraction of sediment transported above Q_{eff} ($f+$, top row) as well as the return interval of Q_{eff} (RI, bottom row) in years as a function of β, C_v, and length of flow record. Contour values represent the median value of $f+$ (top row) and RI (bottom row) of 100 trials of each flow record length.

match the continuous distribution. However, over engineering time frames (often 50–100 years), this is likely not the case. The return interval of Q_{eff} (RI, calculated with equation (3) for median values of Q_{eff} from 100 trials) behaves in a similar manner as $f+$ in terms of the threshold effect in the β direction (Figure 4, bottom row). Here, RI remains fairly constant with β until the threshold is reached. After which RI rapidly jumps to a much larger value as Q_{eff} occurs in the uppermost discharge bins of the effectiveness histograms.

The record length results show that use of a continuous flow PDF inherent in theoretical MFA weights sediment transport to the tails of the flow PDF and overestimates their influence. Theoretical approaches do not capture the variability and sensitivity of MFA to finite flow records, especially for larger C_v and β values. We find that the need for a longer flow record becomes more important as the variability of the flows increases as well as for values of β greater than approximately 2. This demonstrates that caution should be used when calculating effective discharge in systems with shorter flow records and highly variable flow conditions. For example, one relatively large flow event in the right tail of 10 year flow record is the most effective for $\beta = 3$ and $C_v = 1$. While a very infrequent flow may be the calculated effective discharge, consideration should also be given to the effectiveness peak of the more frequent flows, or a range of flows, when designing a channel for sediment continuity.

4.3. Compound Channel Analysis

Next we consider the influence of compound channel form on MFA by using a sediment-discharge rating curve for two cases: (1) a single power law (SPL) function for all discharge values, and (2) a piecewise or broken power law (BPL) function which incorporates a break in the stage-discharge relationship at Q_{bf} to simulate overbank flows.

Using the SPL under case 1, a continuously increasing relationship between $f+$ and C_v is predicted, which coincides with the theoretical solution for $f+$ described by equation (4). However, if we assume that shear stress on the channel bed increases at a slower rate with discharge for overbank flows than for in-channel flows, as with the BPL sediment transport relation in case 2, then a decreasing relationship is predicted between C_v and $f+$ after a peak in $f+$ at $C_v \approx 1.5$–2.0 (Figure 5a). The location of this peak depends on the degree of difference between channel bank slope and floodplain lateral slope. As the value of b_{fp} decreases the lateral floodplain

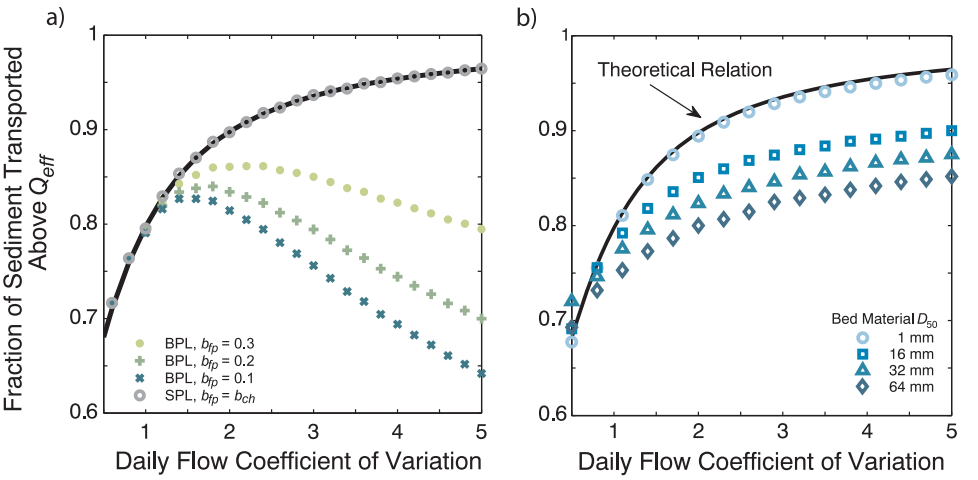

Figure 5. (a) The fraction of sediment transported by discharges greater than Q_{eff}, $f+$, for the single power law (SPL) and broken power law (BPL) at-a-station hydraulic geometry relationships. (b) Values of $f+$ for a range of grain sizes in a noncompound channel using an entrainment threshold for sediment transport.

slope becomes milder relative to the channel bank slope, and the amount of sediment transported at a given overbank discharge decreases. This reduces the relative influence of larger, infrequent flows.

In case 1, Q_{eff} reduces in absolute magnitude with increasing C_v resulting in more sediment being transported at flows greater than Q_{eff} and an increase in $f+$. In case 2, Q_{eff} behaves the same way with C_v since it is less than Q_{bf} where the break in at-a-station overbank hydraulic geometry occurs. For a given value of C_v, $f+$ is smaller in case 2 than in case 1 because less sediment is transported overall by overbank flows. The fraction of sediment transported above Q_{eff} continues to decline with increasing C_v in case 2 as overbank floods become more frequent, but less effective when compared to case 1. This relationship may change if a threshold for sediment transport is introduced, which is explored by itself in the next section.

It is often the case that breaks in stage-discharge relationships are not explicitly incorporated in MFA [e.g., *Andrews*, 1980; *Nash*, 1994]. However, as *Hey* [1996], and others studying the hydraulics of compound channels [e.g., *Knight and Demetriou*, 1983] note, single stage-discharge or stage-shear stress relationships may not accurately capture the hydraulics of natural rivers with floodplains. Of course, the question of capacity-limited sediment transport at large flows is more complex than treated herein. For example, fine sediment-limited systems can develop armor layers [*Dietrich et al.*, 1989], which can lead to discontinuous flow-sediment transport relationships before and after armor layer breakup [*Bathurst*, 1987]. Nevertheless, this

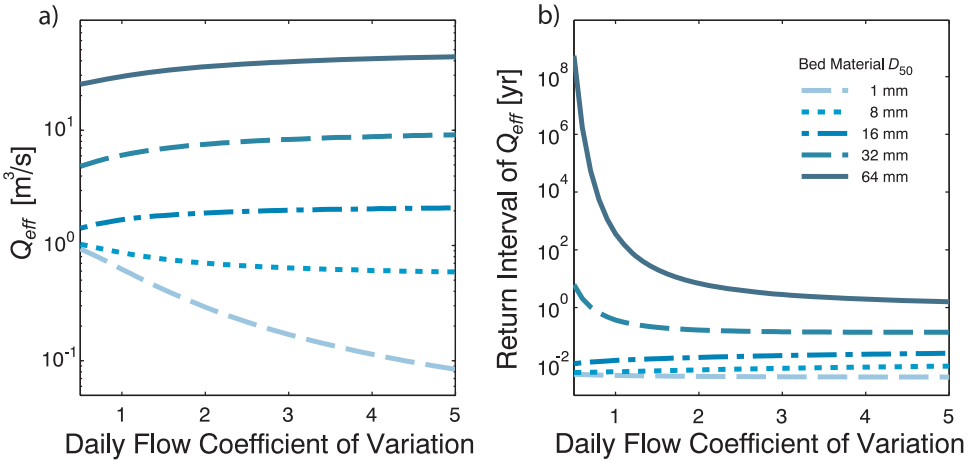

Figure 6. (a) The value of Q_{eff} as a function of C_v and sediment grain size, D_{50}. (b) The return interval of Q_{eff} in years as a function of the same. Note that the $Q_{eff} - C_v$ relationship decreases for relatively small sediment (sand to fine gravel) but increases for large sediment sizes (medium gravel to small cobble).

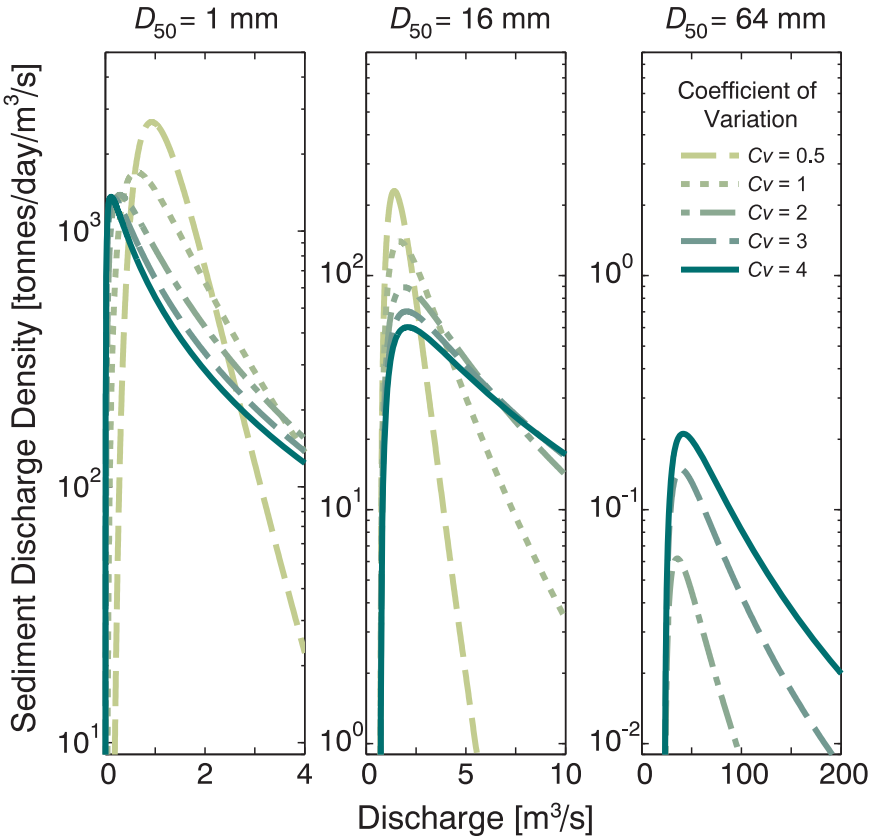

Figure 7. Effectiveness curves for a range of grain sizes and C_v values. Note that the discharge associated with the peaks of these curves, Q_{eff}, decreases with increasing C_v for small grain sizes and increases with increasing C_v for large grain sizes.

simple computational experiment has demonstrated that explicitly incorporating floodplain morphology and overbank flows can substantially influence calculations of the magnitude and frequency of sediment transport in natural rivers. We have shown that flow variability interacts with floodplains to reduce the influence of large infrequent flows on long-term sediment transport in channels.

4.4. Sediment Entrainment Threshold Analysis

The final element of physical context we introduce to the theoretical MFA approach is a threshold for sediment entrainment. Sediment transport operating with a threshold interacts with flow distributions in ways that depart from the simplistic sediment-rating curve. For distributions with low C_v, large flows are relatively rare. Transport of coarse sediment classes—and the most effective discharge for these sediment size classes—occur primarily in the right tail of the flow distribution resulting in a very large *RI* (Figure 6b). With increasing C_v, flows less than the threshold for sediment entrainment become more frequent pushing, the bulk of sediment transport further out into the right tail of the flow distribution and increasing the absolute value of Q_{eff} (Figure 6a). However, as C_v increases in coarse-bedded rivers, *RI* drops precipitously with increasing C_v as the larger flows necessary to move coarser sediment become more common (Figure 6b). In contrast, in fine grain streams with very low or negligible entrainment thresholds the peak of the effectiveness curve follows that of the flow distribution as C_v increases. This means that the absolute value of Q_{eff} decreases with increasing C_v (Figures 6a and 6b; Figure 7, left). This reverse in the relationship between C_v and Q_{eff} between coarse and fine sediment can be seen by examining the peak of effectiveness curves for a range of sediment sizes and C_v values (Figure 7).

We find a reduction in $f+$ as a function of C_v for values generated with the threshold-type sediment transport relation compared to what equation (4) predicts (Figure 5b). This difference increases with grain size. The threshold for fine-grained sediment (1–8 mm in this example) is relatively small and the sediment transport relation for this size class approximates the single power law, sediment-rating curve used in equation

(4). Therefore, the $f+ - C_v$ relationship for sand size material (1 mm) approximates the theoretical relation (equation (4)). However, as sediment size increases ($\geq$ 1 mm in this example), the $f+ - C_v$ relationship increasingly falls below the theoretical relation, though parallels its shape. This is due to the $Q_{eff} - C_v$ relationship previously discussed: as C_v increases more flows occur below the threshold of entrainment for coarser sediment resulting in less sediment transport overall. This combination of effects results in increasingly smaller values of $f+$ as grain size and C_v increase.

The divergence in trends in absolute value of Q_{eff} and C_v between streams with fine versus coarse sediment has been documented in these stream types separately in the literature. Work by *Bunte et al*. [2013] in bed load-dominated gravel and cobble streams suggests that as flow variance increases so does Q_{eff} such that for certain large values of flow variance, Q_{eff} may be the largest discharge on record (assuming that sediment is never supply limited in these streams). In sand bed streams dominated by suspended load, *Soar et al*. [2005] found a decreasing relationship between the ratio Q_{eff}/Q_{bf} and flow variance using a different metric of flow variance: Q_2/Q_{mean}, where Q_2 is the 2 year flood based on the maximum annual flood series and Q_{mean} is the mean annual discharge. Here we present a physical mechanism for this diverging relationship across sediment size classes due to the relationship between flow variability and the magnitude and frequency of flows greater than the threshold for sediment entrainment.

5. Conclusions

Magnitude-frequency analysis (MFA) conducted with theoretical, closed-form equations (2), (3), and (4) provides valuable insight about the general relationships between sediment transport mode, flow variance, and the magnitude of the effective discharge, Q_{eff}, to generate hypotheses about the physical world. However, these theoretical approaches fall short of capturing important physical processes and complexities inherent in rivers and streams, and may not apply to actual river management scenarios, which have finite time horizons. In this study, we have used simple numerical experiments to test the validity of theoretical MFA approaches in predicting the magnitude and frequency of sediment transport. We have also used the analytical framework implicit in these approaches to study the influence of compound channel form and a threshold for sediment entrainment on the magnitude and frequency of sediment transport.

Theoretical MFA relations predict a monotonic increase in the absolute value, as well as the return interval (*RI*), of the effective discharge, Q_{eff}, with increasing flow coefficient of variation, C_v, and sediment-rating curve exponent, β using equations (2) and (3) (Figure 2). The fraction of sediment transported by discharges greater than Q_{eff}, $f+$, as predicted by equation (4), monotonically increases with C_v and approaches unity asymptotically for large values of C_v (Figure 5, solid line).

In this study, we demonstrate that even modest modifications to the assumptions contained in these theoretical approaches result in divergent relationships among flow variance, sediment transport mode, and values of MFA metrics. We find the following:

1. Median values of MFA metrics *RI* and $f+$ from finite flow records sampled from the same continuous flow probability density function used in the theoretical MFA relations demonstrate complex, nonmonotonic, and threshold-driven relationships as a function of C_v, β, and the length of the flow record (Figure 4) not reflected in the theoretical relations for these metrics.
2. Introducing compound channel morphology by creating a break in the stage-discharge relationship at the bankfull discharge causes the $f+ - C_v$ relationship to fall well below that predicted by equation (4). The value of $f+$ increases up to an intermediate value of C_v and then decreases for larger values of C_v (Figure 5a). This outcome is due to the reduction in effectiveness of overbank flows with the existence of a floodplain. It is sensitive to the difference between channel bank slope and floodplain lateral slope.
3. Inclusion of a threshold for sediment entrainment results in a divergent relationship between Q_{eff} and C_v between fine and coarse-grain channels. In channels with fine-grained sediment, the absolute value of Q_{eff} decreases with increasing C_v while the value of $f+$ follows equation (4) closely. In channels with coarse-grained sediment and larger entrainment thresholds, the absolute value of Q_{eff} increases with C_v and the value of $f+$ falls below that predicted by equation (4) (Figures 5b, 6, and 7).

This divergence in the $Q_{eff} - C_v$ relationship for fine versus coarse sediment has been observed separately in coarse-bed [*Bunte et al*., 2013] and fine-bed streams [*Soar et al*., 2005]. As the flow distribution becomes

more positively skewed with increasing C_v smaller flows become more frequent resulting in Q_{eff} reducing with C_v in fine-grained streams with low sediment entrainment thresholds. In coarse-grained streams, these more frequent small flows associated with larger C_v fall below the entrainment threshold. Flows in the tails of the distribution then dominate sediment transport and, because the flow PDF tail thickens with increasing C_v, Q_{eff} also increases.

Magnitude-frequency analysis of sediment transport in rivers provides a process-based, analytical tool for river scientists and managers to characterize what flow or range of flows is most responsible for transporting sediment and maintaining sediment continuity in a channel. These approaches may be applied practically (e.g., channel design and environmental flow studies) and academically (e.g., dynamic equilibrium theory). Our study indicates that the empirical approach to MFA, which is based on a finite flow record, should be relied on for practical questions with engineering time horizons (50–100 years). However, in applying the empirical approach to systems with shorter flow records ($\leq$ 10 years) that have larger C_v values and/or β values ($\geq$ 2), a few large flows can overwhelm MFA resulting in very large estimates of Q_{eff}. Depending on the question of interest, this result may or may not be appropriate to consider in the long-term sediment yield of a river.

Theoretical MFA approaches are useful for predicting general relationships between aspects of the flow regime, sediment transport mode, and sediment yield in research settings. We found that their assumptions limit their use primarily to cases where sediment entrainment thresholds are nonexistent or are very small (e.g., wash or dissolved load) when a sediment rating curve is utilized, where compound channel form is lacking, or where only in-channel flows are considered. The values and behaviors of metrics based on integrals of continuous and infinite PDFs such as $f+$ diverge from those generated from discrete and finite records in large part due to the lack of a continuous right tail in the flow distribution of finite records (Figure 3). This lack of continuity in the right tail of empirical records is of course a phenomenon of sample size. This study indicates that use of a continuous theoretical flow PDF over weights sediment transport in the tails and overestimates their influence under engineering time-frames (often 50–100 years) when compared to empirical distributions of finite flow records.

Future work will more closely consider the interaction between channel form, flow regime, and sediment transport mode. The behavior of MFA metrics using different probability distributions other than the two-parameter lognormal distribution as well as the use of bed load versus total load sediment transport equations will be considered. These and other metrics generated from MFA have the potential to inform general geomorphic theory as well as process-based channel design.

Notation

a	coefficient for at-a-station hydraulic geometry relation. Subscripts "*ch*" and "*fp*" denote in-channel and overbank or floodplain values, respectively.
α	coefficient for sediment transport rating curve.
β	exponent for sediment transport rating curve.
b	exponent for at-a-station hydraulic geometry relation. Subscripts "*ch*" and "*fp*" denote in-channel and overbank or floodplain values, respectively.
C_v	coefficient of variation of daily flows.
D_s	sediment grain size (m). Subscript "50" denotes the median grain size value.
$f+$	fraction of sediment transported by discharges greater than the effective discharge.
k	sediment transport relation coefficient.
μ	mean of untransformed (μ_x) and log-transformed (μ_y) daily flows.
σ	standard deviation of untransformed (σ_x) and log-transformed (σ_y) daily flows.
Φ	cumulative normal distribution function.
Q	discharge rate, m^3/s.
Q_s	sediment discharge rate, tonnes/day.
Q_{bf}	bankfull discharge, m^3/s.
Q_{eff}	effective discharge, m^3/s.
RI	return interval of a discharge value, year.
RL	flow record length, year.
τ^*	Shields dimensionless shear stress. Subscript "*c*" denotes critical value for sediment entrainment.

Acknowledgments
Matlab® code created for this analysis is available upon request. This research was conducted while the first author was a National Science Foundation, Integrative Graduate Education and Research Traineeship I-WATER fellow at Colorado State University. We also gratefully acknowledge support from the Transportation Research Board, National Cooperative Highway Research Program. This paper benefitted from discussions with Richard Vogel, Kristin Bunte, and Jose Salas as well as reviews from John Pitlick and two anonymous reviewers.

References

Ackers, P. (1993), Stage-discharge functions for two-stage channels: The impact of new research, *Water Environ. J.*, *7*(1), 52–59.
Andrews, E. (1980), Effective and bankfull discharges of streams in the Yampa River basin, Colorado and Wyoming, *J. Hydrol.*, *46*(3-4), 311–330.
Andrews, E., and J. M. Nankervis (1995), Effective discharge and the design of channel maintenance flows for Gravel-Bed Rivers, in *Natural and Anthropogenic Influences in Fluvial Geomorphology*, vol. 89, edited by J. E. Costa et al., pp. 151–164, AGU, Washington, D. C.
Archfield, S. A., R. M. Vogel, and S. L. Brandt (2007), Estimation of flow duration curves at ungaged sites in southern New England, in *Proceedings of the ASCE World Environmental and Water Resources Congress*, pp. 1–14, Am. Soc. of Civ. Eng., Tampa, Fla.
Barry, J., J. M. Buffington, and J. G. King (2004), A general power equation for predicting bed load transport rates in gravel bed rivers, *Water Resour. Res.*, *40*, W10401, doi:10.1029/2004WR003190.
Barry, J., J. M. Buffington, P. Goodwin, J. G. King, and W. W. Emmett (2008), Performance of bed load transport equations relative to geomorphic significance: Predicting effective discharge and its transport rate, *J. Hydraul. Eng.*, *134*(5), 601–615.
Bathurst, J. (1987), Modelling and measuring sediment transport in channels with coarse bed material, in *River Channels: Environment and Process*, edited by K. S. Richards, pp. 272–294, Blackwell Sci., Oxford, England, U. K.
Benson, M., and D. M. Thomas (1966), A definition of dominant discharge, *Int. Assoc. Sci. Hydrol. Bull.*, *11*(2), 76–80.
Biedenharn, D., R. R. Copeland, C. R. Thorne, P. J. Soar, and R. D. Hey (2000), *Effective Discharge Calculation: A Practical Guide*, 60 pp., U.S. ACOE-ERDC, Vicksburg, Miss.
Brown, C. (1950), Sediment transportation, in *Engineering Hydraulics*, edited by H. Rouse, pp. 769–857, John Wiley, N. Y.
Bunte, K., S. R. Abt, J. P. Potyondy, and S. E. Ryan (2004), Measurement of coarse gravel and cobble transport using portable bed load traps, *J. Hydraul. Eng.*, *130*(9), 879–893.
Bunte, K., K. W. Swingle, S. R. Abt, and D. Cenderelli (2013), Steep Gravel Bed load Rating Curves Obtained From Bed load Traps Shift Effective Discharge to Flows Much Higher Than "Bankfull," Astract EP41A-0774 presented at 2013 Fall Meeting, AGU, San Francisco, Calif.
Carling, P. (1988), The concept of dominant discharge applied to two gravel-bed streams in relation to channel stability thresholds, *Earth Surf. Processes Landforms*, *13*(4), 355–367.
Dietrich, W., J. W. Kirchner, H. Ikeda, and F. Iseya (1989), Sediment supply and the development of the coarse surface layer in gravel-bedded rivers, *Nature*, *340*(6230), 215–217.
Doyle, M., D. Shields, K. F. Boyd, P. B. Skidmore, and D. Dominick (2007), Channel-forming discharge selection in River Restoration design, *J. Hydraul. Eng.*, *133*(7), 831–837.
Emmett, W., and M. G. Wolman (2001), Effective discharge and gravel-bed rivers, *Earth Surf. Processes Landforms*, *26*(13), 1369–1380.
Goodwin, P. (2004), Analytical solutions for estimating effective discharge, *J. Hydraul. Eng.*, *130*(8), 729–738.
Hey, R. (1996), Channel response and channel forming discharge, *Rep. 6871-EN-01*, 112 p., U.S. ACOE-ERO, Vicksburg, Miss.
Hey, R., and C. R. Thorne (1986), Stable channels with mobile gravel beds, *J. Hydraul. Eng.*, *112*(8), 671–689.
King, J., W. W. Emmett, P. J. Whiting, R. P. Kenworthy, and J. J. Barry (2004), Sediment transport data and related information for selected coarse-bed streams and Rivers in Idaho, *Gen. Tech. Rep. RMRS-GTR-131*, 26 p., USDA, Forest Serv., Rocky Mountain Res. Stn., Fort Collins, Colo.
Klonsky, L., and R. M. Vogel (2011), Effective measures of "Effective" discharge, *J. Geol.*, *119*(1), 1–14.
Knight, D. W., and J. D. Demetriou (1983), Flood plain and main channel flow interaction. *J. Hydraulic Eng.*, *109*(8), 1073–1092.
Knighton, D. (1998), *Fluvial Forms and Processes: A New Perspective*, 2nd ed., 400 p., E. Arnold, London, U. K.
Limbrunner, J. F., R. M. Vogel, and L.C. Brown (2000), Estimation of harmonic mean of a lognormal variable, *J. Hydrol. Eng.*, *5*(1), 59–66.
Mackin, J. (1948), The concept of a graded river, *Geol. Soc. Am. Bull.*, *59*(5), 463–512.
Meyer-Peter, E., and R. Müller (1948), Formulas for bed load transport, in *Proceeding of IAHR 2nd Meeting*, pp. 39–64, IAHR, Stockholm, Sweden.
Nash, D. (1994), Effective sediment-transporting discharge from magnitude-frequency analysis, *J. Geol.*, *102*(1), 79–95.
Nolan, K., T. M. Lisle, and H. M. Kelsey (1987), Bankfull discharge and sediment transport in northwestern California, in *Erosion and Sedimentation in the Pacific Rim*, edited by R. L. Beschta, pp. 439–450, IAHS Publ., Wallingford, Oxfordshire, U. K.
Orndorff, R., and P. J. Whiting (1999), Computing effective discharge with S-PLUS, *Comput. Geosci.*, *25*(5), 559–565.
Parker, G. (1979), Hydraulic geometry of active gravel rivers, *J. Hydraul. Div.*, *105*(9), 1185–1201.
Pickup, G., and R. F. Warner (1976), Effects of hydrologic regime on magnitude and frequency of dominant discharge, *J. Hydrol.*, *29*(1-2), 51–75.
Pitlick, J., Y. Cui, and P. Wilcock (2009), *Manual for Computing Bed Load Transport Using BAGS (Bedload Assessment for Gravel-bed Streams) Software, Gen. Tech. Rep. RMRS-GTR-223*, 45 pp., USDA, USFS Rocky Mt. Res. Sta., Fort Collins, Colo.
Poff, N. (1996), A hydrogeography of unregulated streams in the United States and an examination of scale-dependence in some hydrological descriptors, *Freshwater Biol.*, *36*(1), 71–79.
Quader, A., and Y. Guo (2009), Relative importance of hydrological and sediment-transport characteristics affecting effective discharge of small Urban streams in Southern Ontario, *J. Hydrol. Eng.*, *14*(7), 698–710.
Shiono, K., J. S. Al-Romaih, and D. W. Knight (1999), Stage-discharge assessment in compound meandering channels, *J. Hydraul. Eng.*, *125*(1), 66–77.
Segura, C., and J. Pitlick (2010), Scaling frequency of channel-forming flows in snowmelt-dominated streams, *Water Resour. Res.*, *46*, W06524, doi:10.1029/2009WR008336.
Soar, P., and C. R. Thorne (2001), Channel design for meandering rivers, *ERDC/CHL CR-01-1*, 367 p.,U.S. ACOE, Vicksburg, Miss.
Soar, P., C. C. Watson, and C. R. Thome (2005), Channel-forming flow: Representations and variability, in *EWRI Conference: Impacts of Global Climate Change*, vol. 44, pp. 1–12, Am. Soc. of Civ. Eng., Env. Water Res. Inst., Anchorage, Alaska.
Syvitski, J., M. D. Morehead, D. B. Bahr, and T. Mulder (2000), Estimating fluvial sediment transport: The rating parameters, *Water Resour. Res.*, *36*(9), 2747–2760.
Torizzo, M., and J. Pitlick (2004), Magnitude-frequency of bed load transport in mountain streams in Colorado, *J. Hydrol.*, *290*(1-2), 137–151.
Vogel, R., J. R. Stedinger, and R. P. Hooper (2003), Discharge indices for water quality loads, *Water Resour. Res.*, *39*(10), 1273, doi:10.1029/2002WR001872.
Wolman, M., and J. P. Miller (1960), Magnitude and frequency of forces in geomorphic processes, *J. Geol.*, *68*(1), 54–74.
Yevjevich, V. (2010), *Probability and Statistics in Hydrology*, 2nd ed., 312 p., Water Resour. Publ., Highlands Ranch, Colo.